Flexible lock-in detection system based on synchronized computer plug-in boards applied in sensitive gas spectroscopy

Andersson, Mats; Persson, Linda; Svensson, Tomas; Svanberg, Sune

Published in:
Review of Scientific Instruments

DOI:
10.1063/1.2813346

2007

Flexible lock-in detection system based on synchronized computer plug-in boards applied in sensitive gas spectroscopy

Mats Andersson, Linda Persson, Tomas Svensson, and Sune Svanberg[a)]
Atomic Physics Division, Lund University, P.O. Box 118, S-221 00 Lund, Sweden

(Received 3 July 2007; accepted 22 October 2007; published online 26 November 2007)

We present a flexible and compact, digital, lock-in detection system and its use in high-resolution tunable diode laser spectroscopy. The system involves coherent sampling, and is based on the synchronization of two data acquisition cards running on a single standard computer. A software-controlled arbitrary waveform generator is used for laser modulation, and a four-channel analog/digital board records detector signals. Gas spectroscopy is performed in the wavelength modulation regime. The coherently detected signal is averaged a selected number of times before it is stored or analyzed by software-based, lock-in techniques. Multiple harmonics of the modulation signal ($1f$, $2f$, $3f$, $4f$, etc.) are available in each single data set. The sensitivity is of the order of 10^{-5}, being limited by interference fringes in the measurement setup. The capabilities of the system are demonstrated by measurements of molecular oxygen in ambient air, as well as dispersed gas in scattering materials, such as plants and human tissue. © *2007 American Institute of Physics.*
[DOI: 10.1063/1.2813346]

I. INTRODUCTION

Analog lock-in techniques for tunable diode laser spectroscopy have been used for decades to improve the performance in the detection of trace gases.[1–4] Originally, desktop, lock-in amplifiers were used in combination with mechanically chopped light. Today, external signal generators are used to superimpose sine wave modulation signals on the laser operation current. The modulation signal also acts as phase reference and is fed to an analog, lock-in amplifier. This lock-in amplifier is then capable of filtering out harmonic components generated when light passes an absorbing sample/gas cell. Absorption lines are scanned across by superimposing a low-frequency triangular or sawtooth ramp on the operating current of the laser. The major reason for using lock-in detection is to suppress noise by moving the detection frequency to a range that is normally less affected by noise (above 1 kHz).[5] In the 1980s, modulation techniques such as wavelength-,[6] frequency-,[7] and two-tone frequency[8] modulation schemes were developed. Normally, direct absorption measurements (baseband detection) give a detection limit of 10^{-3}–10^{-4}, while modulation techniques such as wavelength and frequency modulations, give a detection limit of 10^{-6} or better.[9] Over the past 10 years digital amplifiers have been used and, currently, small digital-signal-processing based lock-in solutions are being developed and used.[10,11]

Even if the use in spectroscopy of modulation techniques, based on phase-sensitive detection, is straightforward, it is normally not easy to analyze and probe the raw signal, due to sources of error that affect the gas imprint signal before the lock-in detection has been implemented. This is because the detected gas imprint signal is weak and markedly affected by noise. Thus, data from the lock-in amplifier need to be averaged for several seconds or minutes in order to achieve the needed signal-to-noise ratio (SNR). It is often not possible to average the raw signal without degradation. This is due to unavoidable trigger jitter. Moreover, since lock-in detection normally takes place in real time, another drawback is that the influence of a change in lock-in settings (for example, the selection of harmonic) cannot be evaluated later on. In addition to the lock-in technique, methods to improve the signal include balanced detection,[12] coherent sampling,[13] waveform averaging,[14] and high-pass filtering prior to lock-in detection.[13]

Coherent sampling is a well-known technique, commonly used in spectrum analysis and signal processing for acoustics and telecom research and development. In coherent sampling, a master clock is used to create modulation waveforms and to control the sampling process of the detector signal. Coherent sampling requires that an integer number of wanted waveforms exist in the acquired data set and that the ratios between the sampling and the modulation frequencies (both laser scanning and laser modulation signals) are integers.[15–17] With this technique a number of scanned signals can be averaged before the lock-in detection is carried out. Periodic noise such as power supply ripple and external optical noise from fluorescent lamps, etc., which does not fulfill the requirements above, is averaged out (the coherent sampling process acts as a comb filter) together with nonperiodic noise. It should be noted that coherent sampling facilitates complete postdata processing. For example, this means that applications which previously required several lock-in amplifiers, can now be realized using coherent data acquisition and subsequent harmonic demodulation at desired harmonics (e.g., $1f$ and $2f$). In addition, high-pass filtering can increase the dynamic range further, since it suppresses most of the low-frequency content (e.g., below the $1f$ frequency).

[a)]Electronic mail: sune.svanberg@fysik.lth.se

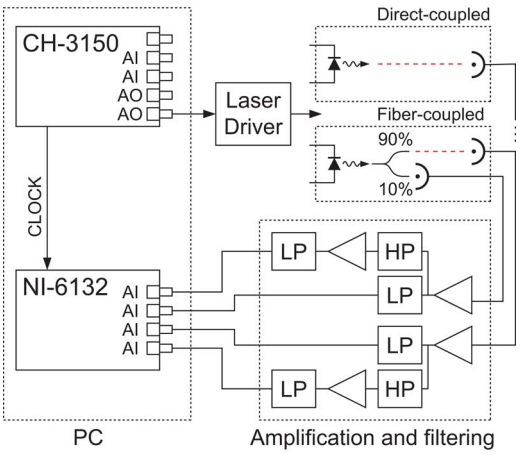

FIG. 1. The direct-coupled and the fiber-coupled experimental setups for measurement on ambient air by the use of VCSEL lasers. The lasers are modulated by an arbitrary waveform that is generated in a data acquisition board (CH-3150, Exacq Technologies). The amplified and high-pass filtered signals from the sample and the reference detectors are sampled coherently and synchronically by a four channel A/D board (NI-6132, National Instruments). See text for more details.

This article describes the construction of a compact and flexible digital lock-in detection system based on two plug-in boards for a standard computer. By employing coherent sampling, raw data storage and postdata processing in the time or frequency domain are made possible. The system can be used for both traditional trace gas analysis, and the more recently introduced high-speed combustion gas analysis requiring scan rates of 100 Hz or more. Experimental arrangements and data acquisition architecture are described in Sec. II. The required analog/digital (A/D)resolution is also discussed. The calibration and applications of the system are presented in Secs. III and IV. Finally, advantages of using a detection system based on coherent sampling and plug-in boards are discussed, and several examples of measurements are given.

II. MATERIALS AND METHODS

A. Optical setup

An overview of the optical setup is shown in Fig. 1. Two different vertical cavity surface emitting lasers (VCSELs) are used alternatingly, and correspond to two different experimental configurations. The *direct-coupled setup* is based on a standard single-mode VCSEL (ULM763-03-TN-S46FOP, Ulm Photonics) with a maximal output of 0.3 mW, operating at 0.25 mW at the sample. The wavelength is scanned across the P11P11 oxygen line at 764.281 nm (vacuum wavelength). The second configuration is referred to as the *fiber-coupled setup*, and employs a pigtailed, single-mode VCSEL (L2K-P760-LD-SM, Laser2000, Sweden) with a maximum output power of 0.2 mW, operating at 0.085 mW at the sample. The wavelength is scanned across the R15Q16 oxygen line at 760.094 nm (vacuum wavelength). After the pigtailed laser, the light is split by a 10/90(%), single-mode fiber splitter (Laser2000, Sweden). The smaller fraction is guided to a reference detector, while the main part is either propagated through ambient air (for calibration purposes, see Sec. III), or guided to a scattering and absorbing sample. A collimating lens package (CFC-5-760, Thorlabs) is used in the case of measurements in ambient air.

The laser frequency is scanned over the absorption lines by ramping the operating current, which is provided by a standard VCSEL current controller (LDC200, Thorlabs). This is done by using a triangular waveform of 130 Hz. A temperature controller (TED200, Thorlabs) ensures general temperature stability. Wavelength modulation is achieved by superimposing a sinusoidal modulation of 133 kHz on the triangular ramping signal. The ramping and modulation signals are created in a peripheral component interconnect (PCI)-based, 12 bit arbitrary waveform generator (CH-3150, Exacq Technologies). Its internal clock is used not only to clock out such waveforms, but also to externally clock the A/D converters (2.496 MHz), via a short coaxial cable, on a second computer board (NI-6132, National Instruments). It is this man euver that implements coherent sampling.

In the fiber-coupled setup, the light beams enter two detectors with built-in transimpedance amplifiers (UDT-455LN, OSI Optoelectronics). In the direct-coupled setup, only one of the above-mentioned detectors is used. In the present case, the gain of the amplifiers is set to 10^3 in order to fulfill a bandwidth of about 1 MHz. Both the sample and the reference signals are amplified by a factor of up to 1000 by an external amplifier in order to minimize external noise and for full utilization of the dynamic range of the AD converter. The reference and the sample signals are also filtered by a second-order, high-pass filter (50 kHz cutoff frequency), and amplified once more by a factor of 100. Measurements on scattering samples, such as bamboo or human tissue, require a large-area detector due to the fact that incident light is scattered and absorbed by the sample. In this case, the default sample detector is replaced by a cooled, large-area ($\varnothing = 10$ mm) avalanche photodiode (APD) module (SD 394-70-72-661, Advanced Photonix).

The advantage of using wavelength modulation techniques was estimated by measuring the relative intensity noise (RIN) of the direct-coupled laser and comparing the noise floor level at low frequency and at the laser modulation frequency. RIN is defined in a 1 Hz bandwidth, and expressed in decibels, as

$$\mathrm{RIN} = 20 \log_{10} \frac{V_{\mathrm{noise}}}{V_{\mathrm{average}}},$$

where V_{noise} is the spectral noise root-mean-square (rms) voltage and V_{average} is the averaged rms voltage corresponding to the averaged optical power recorded at the optical detector.[18] The RIN measurement was done by measuring the noise spectrum of the recorded detector signal with the laser turned on without any modulation or ramp signal. As shown in Fig. 2, the noise level at 133 kHz is about 20 dB (ten times) lower than the low-frequency noise level and gives information on the expected improvement in performance when the wavelength modulation technique is used. The decrease in the performance of a tunable diode laser system based on direct detection is due to flicker noise from the laser. In Fig. 2 the dynamic range achieved is about 126 dB (2.0×10^6) at 133 kHz frequency. According to the data

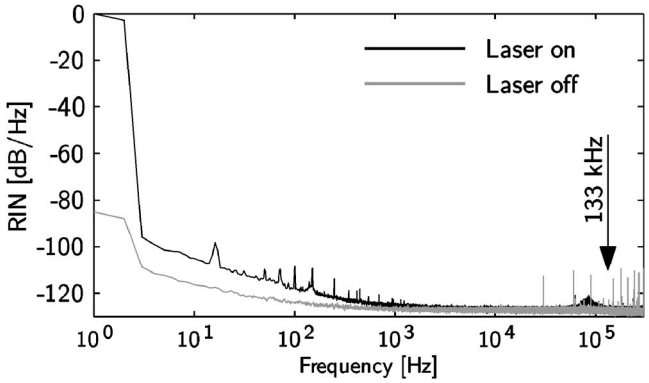

FIG. 2. Laser relative intensity noise (RIN) measurement with a spectral resolution of 1 Hz. Sensor data are recorded by a 14 bit data acquisition card at 600 kS/s over 100 s. The figure shows a power spectrum (RIN measurement) of the recorded detector data with and without unmodulated laser light turned on.

sheet of the laser the RIN value at 1 GHz is about −120 to −130 dB/Hz which sets the performance limit of a spectroscopy system based on this laser. As can be seen in the figure, any further improvement of the dynamic range is limited by the 14 bit data acquisition card since the noise floor is almost the same when the laser is turned off. Further, a detection limit of 10^{-6} requires the system to have a dynamic range of about 120 dB (1×10^{6}). To be able to resolve such a weak signal, a high-pass filter is mounted close to the detector to suppress any signal below the modulation frequency.

B. Data acquisition

A software program, based on LabVIEW, controls the arbitrary waveform acquisition board (CH-3150). First, the scanning and modulation signals to the laser are created and loaded to the board. During the run, the computer central processing unit (CPU) is free to carry out other tasks since the workload of the arbitrary waveform generator is handled by the board itself. All signals are sampled synchronously and coherently to the laser modulation waveforms by the externally clocked, four channel, 14 bit A/D converter PCI board (NI-6132). Sample data blocks that correspond to one scan are added in a data vector created in LabVIEW. Normally, 130 7800 scans (1–60 s) are carried out before averaged data, which are vector data divided by the number of scans, are stored on disk and/or are lock-in detected in the computer by a lock-in detection software module (LOCK-IN toolkit for LabVIEW, National Instruments). The phase reference, used by the lock-in detection module, is created by software. The first and the second channels record the signals from the sample detector (raw signal and high-pass filtered raw signal), while the third and the fourth channels record the signals from the reference detector (reference signal and high-pass filtered reference signal). These two last channels are used only in the fiber-coupled setup; see Fig. 1.

To illustrate the potential of a digital lock-in detection system, based on wavelength modulation and coherent sampling, a measurement based on the direct-coupled setup was performed over a distance of 10 cm in ambient air. Figure 3(a) presents the direct signal recorded, where the

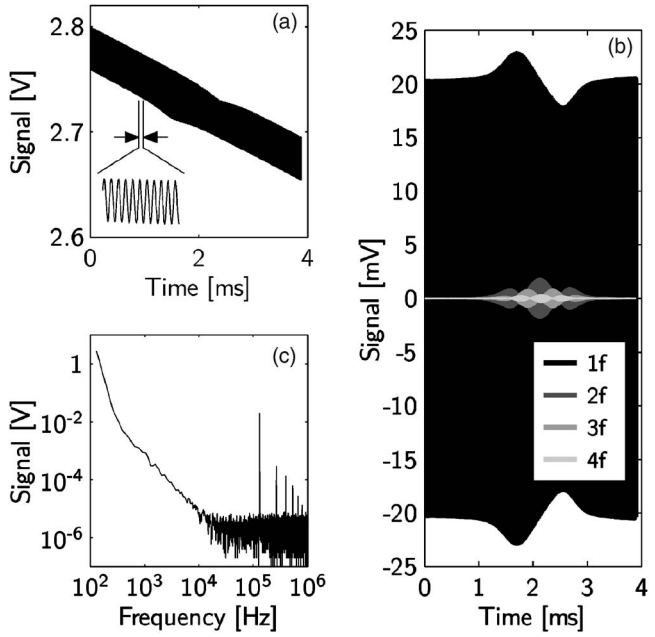

FIG. 3. Typical behavior of the recorded signal for a measurement of oxygen, based on wavelength modulation techniques, for 10 cm of air; 130 (1*s*) synchronous averages. (a) shows the signal from the detector when the laser is scanned about 25 GHz, (b) shows the bandpass-filtered detector signals (three-pole Butterworth, 4 kHz bandwidth) of the detector signal, (c) shows the spectral peak voltages based on an FFT of the detector signal presented in (a). The spectral resolution of the FFT is 130 Hz. See text for more details.

residual amplitude modulation (RAM) signal is clearly seen as a sine wave signal that is present during a scan.[20] The RAM signal occurs because the change in frequency is caused by a change in diode driving current and so altering the output power of the diode laser. In the middle of the frequency scan, the absorption line (P11P11) is crossed, resulting in amplitude changes of the direct signal, and overtones are created ($2f,3f,4f,\ldots$). The amplitude of the RAM signal (40 mV_{pp}) is about 1.5% of the dc level of the signal (2.7 V). The recorded, direct signal was filtered by four software-based, bandpass filters (center frequency at $1f$, $2f$, and $4f$) and the data are presented in Fig. 3(b). This figure shows that the $2f$ signal (4 mV_{pp}) is weaker than the $1f$ signal (6 mV_{pp}) but still of similar amplitude compared to the dip in the direct signal since the amplitude of the $2f$ signal is about 0.1% of the amplitude of the direct signal. The amplitude of the harmonic signals is highly dependent on the modulation index that in this case is set to 2.2.[6] The modulation index is the ratio between the modulation excursion in frequency and the half width at half maximum of the absorption feature. The expected fractional absorption can be used to calculate the dynamic range of the system required. The absorption fraction for 10 cm of air corresponds to 2.45×10^{-3}. It is also shown that the $3f$ and $4f$ signals (1.8 mV_{pp}, respectively, 0.7 mV_{pp}) are weak and that the RAM signal is strong compared to the peak to peak of the $1f$ signal.

To get an overview of the signal spectrum recorded, a fast Fourir transform (FFT) of the data presented in Fig. 3(a) was carried out and is presented in Fig. 3(c). The figure shows that the $1f$ signal (20 mV_{pp} at 133 kHz) is about a

factor of 100 weaker than the averaged signal from the detector (2.7 V). It is also shown that the system SNR, for 130 averages, is about 3×10^5. The SNR is measured at 133 kHz and with a measurement bandwidth of 130 Hz. Normally, SNRs are expressed on a logarithmic (dB) scale according to

$$\mathrm{SNR} = 20\log_{10}\frac{V_{\mathrm{signal}}}{V_{\mathrm{noise}}},$$

where V_{signal} is the averaged detector rms voltage level and V_{noise} is the rms voltage level of measured noise. A SNR of 3×10^5 corresponds to a SNR of about 110 dB. If a high-pass filter is introduced, which suppresses signals below the $1f$ frequency, the A/D dynamic range required decreases by a factor of about 100, as shown in Fig. 3(c).

C. The impact of the A/D converter resolution

The direct-coupled setup was used to study the impact the resolution of an A/D converter has on a coherent measurement system for spectroscopy. A number of streaming and scanning $2f$ detection measurements were performed for a distance in ambient air of 10 mm. This corresponds to a fractional absorption of 2.45×10^{-4}. Four measurements, each recording for 1 min (7800 scans) were done. The sample signal and high-pass sample signal were streamed to a hard disk at 2.469 MS/s. Raw data were stored for each measurement, with different resolutions corresponding to 8, 10, 12, and 14 bits of the A/D converter. By default, the A/D board has a 14 bit resolution but this can be decreased by software during a streaming measurement (based on an application example provided by National Instruments). Thus, the impact of different A/D converter resolutions could be studied. The streamed data were read from the disk, averaged, and lock-in detected. In Fig. 4 the $2f$ signals for a resolution of 8 and 14 bits are presented.

As can be seen on the left-hand side of Fig. 4 and 8 bit A/D converter cannot resolve the oxygen absorption line even though 100 averages are performed. An absorption dip of 2.45×10^{-4} requires a dynamic range of the A/D converter of about 72 dB $[20\log(1/2.45\times10^{-4})]$ to reach an SNR of unity. However, an 8 bit A/D converter has a dynamic range of only about 48 dB and this is too poor to resolve absorption lines in this test setup even though long time averaging is used. If more bits are used the absorption dip can be resolved, even with few or no data averages. 14 bits are enough to resolve an absorption dip of 2.45×10^{-4} since its theoretical dynamic range is about 86 dB. The 100 averages increase the dynamic range by an additional factor of 10 (20 dB).

The performance can be increased by the use of dithering[21] or high-pass filtering,[19] as shown on the right-hand side of Fig. 4. It can be seen that similar performance is reached regardless of whether an 8 bit or a 14 bit AD converter is used. If high-pass filtering is used it should be possible to detect a weak absorption line $(1\times10^{-6}-1\times10^{-8})$ by using a 14 bit or a 16 bit A/D converter. On the right-hand side of Fig. 4, it can also be seen that single scan data are not *a priori* improved by introducing more bits. This is due to the fact that data from one scan are greatly affected by mechanical vibrations introduced by vibration motors. Small vibration motors are mounted in the test setup in order to shake the laser and the detector to minimize persistent optical fringe generation, a well-known detrimental factor in diode laser spectroscopy.[22]

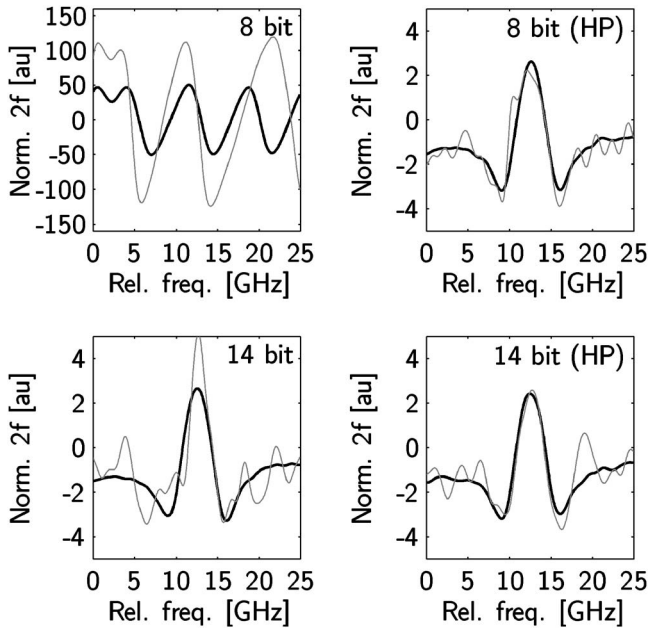

FIG. 4. Streaming measurements on 1 cm of ambient air (fractional absorption of 2.45×10^{-4}) with the direct-coupled setup based on different A/D resolutions and signal filtering. The $2f$ signal for the P11P11 oxygen line at about 764.3 nm is measured for two different average settings: 1 (gray line) and 100 averages (black line). On the left, the $2f$ signal, based on $2f$ detection of the sample signal, is shown for different A/D resolutions and measurement times. On the right, similar data based on $2f$ lock-in-detected, high-pass filtered, sample signals are shown.

III. CALIBRATION OF THE SYSTEM

The standard addition method was used to calibrate and to test the linearity and noise behavior of the system. The method is based on adding a known distance through ambient air between the laser and the detector and monitoring the amplitude of the $2f$ signal, divided by the dc level of the direct signal.[22] The signal increases linearly as is also shown in Fig. 5. The estimated air offset of 4 mm, in the direct-coupled setup, is due to the fact that it is not possible to mount the detector directly connected to the laser in the direct-coupled setup. The estimated air offset of 14 mm in the fiber-coupled setup is due to air inside the collimator package used. It is possible to evaluate $1f$–$4f$ signals from one measurement data file, since data are recorded synchronously almost 20 times for each period of the modulation signal. The figure also shows typical recorded signals of the $2f$ signal for a distance through air of about 35 mm for the fiber-coupled and the direct-coupled setups. As shown in Fig. 5(b), the $2f$ sample signal in the fiber-coupled setup is markedly distorted. The distortion is due to optical interference effects which occur frequently in pigtailed lasers. Periodic noise and fringes can be handled by using balanced detection.[22] By detecting both the sample and reference beams synchronously, a balanced $2f$ detection signal is evaluated, as shown in Fig. 5(b).

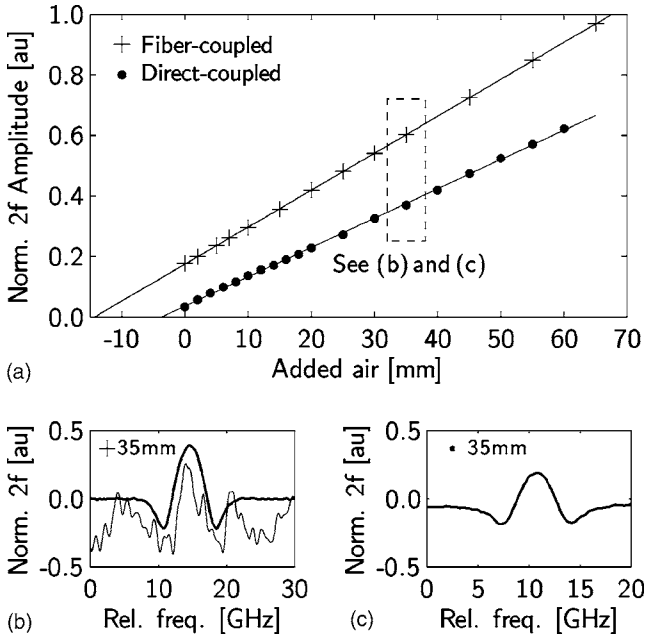

FIG. 5. (a) Standard addition measurement results from the direct-coupled and fiber-coupled measurement setups. Ten measurements (20 s measurement time) were made at each air distance, ranging from 0 to 65 mm. (b) Typical behavior of the $2f$ signal in the fiber-coupled setup for a distance through air of about 35 mm. The figure shows the $2f$ signal of the sample signal (thin line) and the evaluated balanced signal (bold line). (c) Typical behavior of the $2f$ signal in the direct-coupled setup for a distance through air of about 35 mm.

IV. APPLICATIONS

A. Gas discharge measurements on a bamboo stalk

To show the strength of using the digital lock-in detection system, we performed test measurements. The oxygen content inside a bamboo stalk was measured. Similar studies on wood have been carried out previously, using a traditional spectroscopy setup, based on desktop analog lock-in amplifiers.[23,24] The purpose of our measurements was to show how the hollow compartment inside a bamboo stalk interacts with ambient air. The stalk of a bamboo consists of hollow, jointed compartments. We performed measurements on a 23 cm long stalk with an inner diameter of 11 mm. The external diameter was approximately 18 mm. Before the measurement was started, the bamboo stalk was exposed to a nonambient gas by placing it for 72 h in a bag containing nitrogen. Figure 6 shows the direct-coupled setup measurement arrangement and also the experimental data, showing that the discharge of nitrogen has a time constant of about 30 min.

The light reaching the APD detector is in the range of only 0.3 μW or 0.1% of the emitted light from the laser. Initial measurements showed noisy signals, and no pure $2f$ signal could be detected for 20 s of averaging. This is due to interference fringes that appear between the laser, the bamboo stalk, and the detector. Small vibration motors were mounted on the laser and the detector in order to shake the test setup to minimize persistent fringe generation that otherwise overrides the $2f$ oxygen signal. Even though each measurement point in Fig. 6 is based on 20 s of averaging (2600 scans), measurement data still fluctuate. This could be

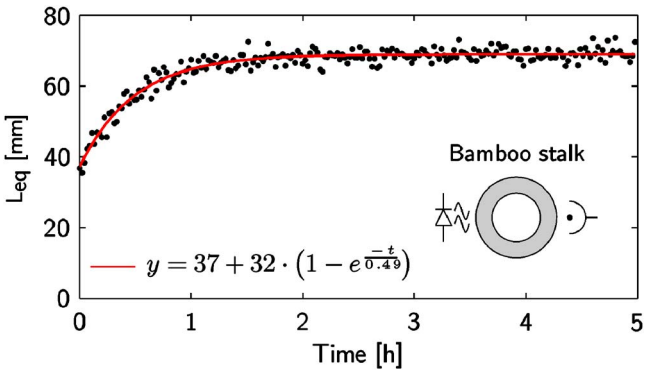

FIG. 6. (Color online) Measurement on nitrogen discharge in a bamboo stalk with a diameter of 18 mm. As shown in the figure, the $2f$ signal starts at an offset that corresponds to 37 mm of ambient air. This is partially because the stalk is mounted at a certain distance from the laser and the detector. Thus, light also passes through ambient air, not only through the stalk.

the result of changing motor speed, backscattered light, interference fringes, etc., which add noise and intensity fluctuations.

B. Measurements on the human frontal sinus

Human frontal sinuses are air-filled cavities in the frontal bone. Measurements on these sinuses, on a healthy volunteer, were performed with the fiber-coupled setup. This setup was chosen since the measurement requires a device that can be positioned at any point on the human body. The tip of the fiber was positioned onto the caudal part of the frontal bone while the APD detector was positioned on the forehead about 3 cm from the fiber. The light that reaches the APD detector was in the range of only 0.15 μW or 0.2% of the emitted light from the laser. Measurements, based on 60 s of averaging, show a $2f$ signal that corresponds to an distance through ambient air of 13 mm. The result is in agreement to that reported in Ref. 25. As expected, the SNR of the $2f$ signal is

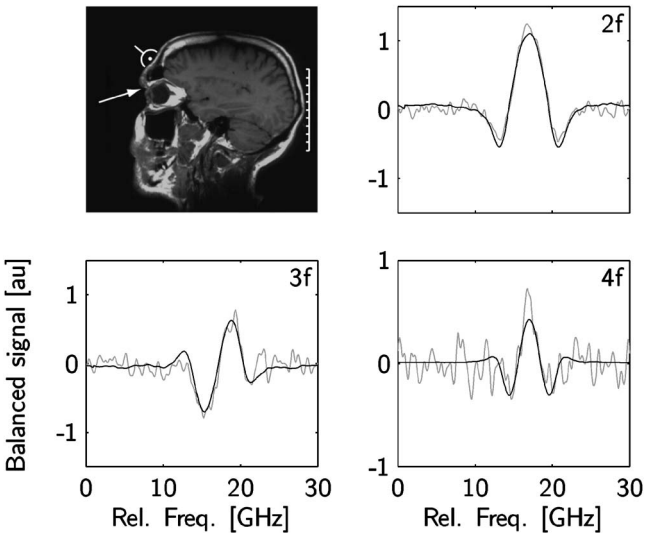

FIG. 7. Measurement on frontal sinuses on a healthy volunteer. The strength of the signal corresponds to a distance through ambient air of 13 mm. The figure shows the behavior of the $2f$–$4f$ signals for one measurement (60 s averaging). See text for more details.

higher than for the $3f$ and $4f$ signals, as shown in Fig. 7. The measurement time, to produce a signal of an acceptable signal, should be 10–30 s. Commonly, fringes dominate the noise floor and in some cases the $4f$ signal contains less such noise than the $2f$ signal.[26] Thus, the $4f$ signal may be a better choice for data analysis in the case of large interference fringes. However, the $4f$ analysis requires more light or less attenuation by the sample. This is due to the fact that the signal level of the $4f$ signal is lower than the $2f$ signal by a factor of 5, as shown in Fig. 3.

V. DISCUSSION

The CH-3150 board was chosen because it has a fast arbitrary generator onboard, which can be used to modulate the laser. Any modulation frequency from dc to several megahertz can be created without loading the computer central processor unit (CPU). The two analog input channels onboard can be used to coherently sample the detector signals at the same time. Thus, this board would be adequate to develop a flexible, powerful, cheap, and compact system for trace gas analysis. This system can be used in general gas spectroscopy and in applications with fast changing environments such as in combustion, requiring a ramping frequency of the order of 1 kHz. However, since four input channels were required for balanced detection to suppress fringes, a second board was introduced (NI-6132) that contains four synchronized A/D converters clocked by the CH-3150 board. The clock signal and the waveform sync signal were fed to the A/D board via two coaxial cables mounted inside the computer. This action was taken to suppress noise and prevent cross-talk between the clock and the detector signals.

Even though this system can be run incoherently, like an ordinary, personal computer (PC)-based, lock-in detection system, coherent sampling is used since this avoids the requirement that lock-in data are real-time data. Data can thus be averaged in real time coherently and can be processed after the averaging is finished or stored for later analysis. The user is free to analyze the data in the time or the frequency domain. This provides the possibility of analyzing signals from several channels and performing baseband analysis and lock-in detection ($1f$–$4f$) on the same data set. The current solution corresponds to the performance of standardized, digital lock-in amplifiers. However, with this setup, baseband detection, $1f$–$4f$ detection, and fast ramp frequencies (4 Hz–1 kHz) could be used by running different software applications without any changes having to be made in the hardware. The solution is compact and installed in an ordinary PC.

If higher performance is needed, high-pass filtering of the detector signal increases the dynamic range of the signal detection, since most of the low-frequency signals (below $1f$) are thus suppressed. When this technique is used, the resolution requirement of the A/D converter is not critical. A 12–16 bit A/D converter should be adequate even for applications requiring a fractional absorbance of about 1×10^{-7}. The output resolution of the D/A converter is 12 bits, which adds quantization noise even though the CH-3150 board has analog reconstruction filters onboard. It is difficult to estimate how this limitation affects the resolution of the system since amplitude noise at the laser input is converted into amplitude and frequency variations in the laser at the same time.

Another way to improve the performance of the system is to replace the current data acquisition (DAQ) boards with boards with higher resolution. As an example, a second measurement was performed to measure the laser noise using a 24 bit data acquisition board (NI-4472, National Instruments). The use of this board resulted in lowering the noise floor at 10 kHz by an additional 30 dB. However, this board is too slow (about 100 kHz sampling frequency) for combustion measurements, for instance, and it is not possible to clock it externally. Thus, this board cannot be used in a coherent sampling system. It is also possible to add input channels by replacing the A/D board with a board with eight input channels, for example. If a cheaper solution is needed, standardized external sound cards can be used. Today, these devices have excellent performance with 24 bit resolution A/D and D/A converters. The only drawbacks are that the sampling clock is limited to 196 kHz and no dc level can be measured. However, this solution may be adequate for some applications.

VI. SUMMARY

By the use of plug-in boards for standardized computers, a powerful and flexible detection system for gas spectroscopy was developed. One of the greatest advantages of the system is that raw data, from a number of channels, can be streamed and stored on disk by the use of standardized software. There is no need for specially designed computers, field-programmable gate arrays, or embedded solutions. Coherent sampling allows the raw data to be analyzed in real time or postprocessed in the time or frequency domain. In our experience the current system is limited by interference fringes in the optical setup.

ACKNOWLEDGMENTS

This work was supported by the Swedish Research Council and the Knut and Alice Wallenberg Foundation. The authors are grateful for Lars Rippe for sharing his expertise in measurement technology.

[1] P. Werle, Spectrochim. Acta, Part A **54**, 197 (1998).
[2] G. Galbács, Appl. Spectrosc. Rev. **41**, 259 (2006).
[3] M. Allen, Meas. Sci. Technol. **9**, 545 (1998).
[4] K. Song and E. C. Jung, Appl. Spectrosc. Rev. **38**, 395 (2003).
[5] D. T. Cassidy and J. Reid, Appl. Opt. **21**, 1185 (1982).
[6] J. Reid and D. Labrie, Appl. Phys. B: Photophys. Laser Chem. **26**, 203 (1981).
[7] G. C. Bjorklund, Opt. Lett. **5**, 15 (1980).
[8] D. T. Cassidy and J. Reid, Appl. Phys. B: Photophys. Laser Chem. **29**, 279 (1982).
[9] J. Silver, Appl. Opt. **31**, 707 (1992).
[10] R. Alonso, F. Villuendas, J. Borja, L. A. Barragn, and I. Salinas, Meas. Sci. Technol. **14**, 551 (2003).
[11] A. Gnudi, L. Colalongo, and G. Baccarani, Proceedings of the European Solid-State Circuits Conference, 1999 (unpubished).
[12] P. Vogel and V. Ebert, Appl. Phys. B: Lasers Opt. **72**, 127 (2001).
[13] T. Fernholz, H. Teichert, and V. Ebert, Appl. Phys. B: Lasers Opt. **75**, 229 (2002).
[14] P. Werle, R. Miicke, and F. Slemr, Appl. Phys. B: Lasers Opt. **57**, 131

(1993).
[15] R. Rosing, H. Kerkhoff, R. Tangelder, and M. Sachdev, J. Electronic Testing: Theory and Applications **14**, 67 (1999).
[16] P. Heinonen, T. Saramaki, J. Malmivuo, and Y. Neuvo, IEEE Trans. Circuits Syst. **31**, 438 (1984).
[17] M. E. Takanen, Ph.D. Thesis, Helsinki University of Technology, 2005.
[18] C. Thibon, F. Dross, A. Marceaux, and N. Vodjdani, IEEE Photon. Technol. Lett. **17**, 1283 (2005).
[19] R. Engelbrecht, Spectrochim. Acta, Part A **60**, 3291 (2004).
[20] X. Zhu and D. T. Cassidy, J. Opt. Soc. Am. B **14**, 1945 (1997).
[21] J. Reid, M. El-Sherbiny, B. K. Garside, and E. A. Ballik, Appl. Opt. **19**, 3349 (1980).
[22] L. Persson, F. Andersson, M. Andersson, and S. Svanberg, Appl. Phys. B: Lasers Opt. **87**, 523 (2007).
[23] M. Sjöholm, G. Somesfalean, J. Alnis, S. Andersson-Engels, and S. Svanberg, Opt. Lett. **26**, 16 (2001).
[24] J. Alnis, B. Anderson, M. Sjholm, G. Somesfalean, and S. Svanberg, Appl. Phys. B: Lasers Opt. **77**, 691 (2003).
[25] L. Persson, M. Andersson, M. Cassel-Engquist, K. Svanberg, and S. Svanberg, J. Biomed. Opt. **12**, 053001 (2007).
[26] P. Kluczynski and O. Axner, Appl. Opt. **38**, 5803 (1999).